


Cite this: *RSC Adv.*, 2020, 10, 45189

Received 12th September 2020  
Accepted 11th December 2020

DOI: 10.1039/d0ra07820d

rsc.li/rsc-advances

# cheML.io: an online database of ML-generated molecules†

Rustam Zhumagambetov,<sup>†a</sup> Daniyar Kazbek,<sup>‡a</sup> Mansur Shkipov,<sup>‡a</sup> Daulet Maksut,<sup>a</sup> Vsevolod A. Peshkov<sup>‡\*b</sup> and Siamac Fazli<sup>‡\*a</sup>

Several recent ML algorithms for *de novo* molecule generation have been utilized to create an open-access database of virtual molecules. The algorithms were trained on samples from ZINC, a free database of commercially available compounds. Generated molecules, stemming from 10 different ML frameworks, along with their calculated properties were merged into a database and coupled to a web interface, which allows users to browse the data in a user friendly and convenient manner. ML-generated molecules with desired structures and properties can be retrieved with the help of a drawing widget. For the case of a specific search leading to insufficient results, users are able to create new molecules on demand. These newly created molecules will be added to the existing database and as a result, the content as well as the diversity of the database keeps growing in line with the user's requirements.

## 1 Introduction

### 1.1 Motivation

In the 21<sup>st</sup> century, humankind will face many challenges in science and biomedicine that will require extensive discovery of new molecules and materials.<sup>1–5</sup> When setting new goals associated with molecular design and synthesis, one should keep in mind that the fraction of “chemical space” explored to date is practically infinitesimal – less than one part of 10<sup>5</sup>.<sup>6</sup> At the same time, the existence of vast unexplored molecular horizons suggests that future major scientific tasks could be solved by finding optimal paths to the uncharted areas of chemical space and efficient ways to populate them.

While the discovery of particular molecules, for example penicillin, can have a monumental impact on human society, unfortunately, the creation of novel drugs remains a very complex problem. Making and testing new compounds is a costly and time-consuming process since the number of potential candidates is overwhelming. A standard drug discovery campaign involves two very tedious processes that are high-throughput screening of available/accessible libraries of small molecules and subsequent hit-to-lead optimization. Considering that the “small molecule universe” (SMU), the set of all synthetically feasible organic molecules of 500 Da molecular weight or less, is estimated to contain over 10<sup>60</sup>

structures,<sup>6,7</sup> an exhaustive search for active hits becomes fairly impractical.

Thus, it is desirable to develop appropriate computational tools to narrow down this enormous area of search. Therefore, virtual screening has become an increasingly popular strategy to mine for promising molecules among millions of existing and billions of virtual molecules.<sup>8–10</sup> In the ideal case of computer-aided *de novo* drug design, the computer algorithms have to (i) create molecules, (ii) range them and assess their feasibility, (iii) perform conformational analysis, and (iv) identify the molecules, featuring specific structural properties that are responsible for the affinity towards certain biological receptors.<sup>11,12</sup>

Recently, computational methods have been well adopted by both chemical and pharmaceutical industries. The creation and development of mathematical tools, such as Machine Learning (ML) and in particular Deep Learning (DL) algorithms in combination with increased computational resources at a reduced price, contribute to further advances within the fields of materials design, drug discovery, and beyond.<sup>13–17</sup>

Therefore, we set a goal to implement, validate, and compare the molecular outputs of a number of recently established ML algorithms for *de novo* molecule generation. As a result, we created a unified database of virtual molecules in browse-able format – cheML.io.<sup>18</sup> The resulting library has been incorporated into a web-page with a built-in drawing widget allowing to conduct substructure and similarity searches. In addition, a number of calculated molecular properties, such as molecular weight, log *P*, number of H-acceptors/donors, and number of rotatable bonds, among others are accessible for each database member. Thus, researchers across all domains of chemical and biological sciences can witness how the rapidly growing field of

<sup>a</sup>Department of Computer Science, School of Engineering and Digital Sciences, Nazarbayev University, Nur-Sultan, Kazakhstan. E-mail: siamac.fazli@nu.edu.kz

<sup>b</sup>Department of Chemistry, School of Sciences and Humanities, Nazarbayev University, Nur-Sultan, Kazakhstan. E-mail: vsevolod.peshkov@nu.edu.kz

† Electronic supplementary information (ESI) available. See DOI: 10.1039/d0ra07820d

‡ These authors contributed equally to this work.



ML technology can assist in the task of hit identification.<sup>19</sup> Not only does our framework offer the possibility of retrieving the whole set of ML-generated molecules and employ them for virtual screening campaigns, but also new molecules can be generated on demand in a structural similarity driven fashion.

## 1.2 A general introduction to machine learning

Generative machine learning frameworks for the creation of molecular libraries can be roughly classified into three categories and are based on autoencoders,<sup>20</sup> recurrent neural networks (RNNs)<sup>21</sup> and generative adversarial networks (GANs).<sup>22</sup>

The idea of autoencoders can be traced back to the 80s.<sup>20,23</sup> Autoencoders are neural networks that consist of an encoder and a decoder that tries to reconstruct the input. The encoder transforms the input into a compressed vector representation and the decoder attempts to recover the input from this compressed representation. A hidden layer with a limited number of nodes between the encoder and decoder represents the minimal amount of information that is needed to decode the original input. Such architectures can be used for denoising, dimensionality reduction and have more recently also been applied for drug discovery.<sup>24</sup>

Recurrent neural networks have been studied for more than 30 years.<sup>21</sup> RNNs consist of several nodes that form a directed graph. In addition to processing input, they also receive their earlier outputs as an input. The output is, therefore, recurring as input in every time step. Applications of RNNs encompass data domains, where input data is “sequentially connected”, like natural language processing, music generation, text translation, automatic generation of image captions, among others.

Generative adversarial networks are a recently established framework for estimating generative models *via* an adversarial process.<sup>22</sup> These types of models have been described as being “the most interesting idea in the last 10 years in Machine Learning” by Yann LeCun. Since their original publication in 2015, they have sparked a huge interest of the scientific community and led to a large number of interesting applications, such as image and video generation,<sup>25–27</sup> music generation,<sup>28</sup> tumor detection,<sup>29</sup> generation and design of DNA<sup>30</sup> as well as novel approaches for computational chemistry,<sup>31,32</sup> namely the generation of new molecules with desired properties. GANs are designed as a zero sum game between two players (*i.e.* machine learning models): the discriminator D and the generator G. An artificial conflict is created between the two players that forces both players to get better throughout the game. D is a deep neural network that acts as a classifier. It looks at some input and will decide, whether this input is real or fake. The generator will take random noise and transforms it to produce outputs that resemble the training data. During the early stages of the game, the generator will not produce realistic outputs and the discriminator is trained to reject these kinds of images. However, G is trained to generate outputs that will fool D into believing his outputs are real. In terms of game theory, a Nash equilibrium is reached, when the generator has recovered the training distribution. At the Nash equilibrium, the best

D can do is guess randomly and G can perfectly reproduce the training data. Since their original publication, there has been tremendous activity within this area of ML.

## 1.3 Digital representations of molecules

In order to apply machine learning tools for molecular generation, a means of encoding the molecules into a suitable digital representation is required.<sup>33</sup> First, molecular structures need to be converted to line notations such as simplified molecular input line entry system (SMILES), Wiswesser Line Notation (WLN), or SYBYL Line Notation (SLN) formats.<sup>34,35</sup> Then, these line notations are transformed into digital representations such as numerical vectors or graphs. Below we outline two common approaches for converting SMILES notations into the input for the machine learning algorithms.

**1.3.1 SMILES strings to vector representation.** Findings of Grzybowski and coworkers<sup>36</sup> implies that SMILES strings can be utilized for (generative) machine learning models by the following general approach. First, a language is constructed by examining the characters the SMILES strings are comprised of. Then, each character or token of the language is assigned to a unique number. Next, numerical vectors are encoded by matching the characters of the SMILES strings with the associated numbers of the language. Finally, these resulting numerical vectors are used as a direct input for training the machine learning algorithms. Such an approach is among the most common for creating digital molecular representations and can be used for ML algorithms that are based on GANs,<sup>32</sup> autoencoders,<sup>37</sup> as well as recurrent neural networks (RNN).<sup>38</sup>

**1.3.2 SMILES strings to graphs.** This approach takes advantage of the resemblance of molecules and graphs. Atoms are represented as vertices and bonds are the edges between them. An otherwise common approach would be the translation of molecules atom by atom. However, this would lead to chemically invalid intermediaries. So, Jin *et al.*<sup>39</sup> proposed a method for encoding and decoding the molecules into graphs in two phases. In the first step, a junction tree is extracted from a given molecule and functions as a scaffold of subgraph components. These components are then used as building blocks for creating new molecules.

## 1.4 Overview of machine learning methods for molecular generation

To populate the database with ML-generated virtual molecules, we have implemented several machine learning frameworks. As we have mentioned previously, existing machine learning methods for molecular generation can be roughly divided into three major categories: GAN-based methods, autoencoder-based methods, and RNN-based methods. Excellent reviews providing comprehensive analysis of all available methods to date have recently appeared in the literature.<sup>14,15</sup> Below we provide a brief description of several machine learning frameworks that we have utilized to populate our database of ML-generated molecules. A graphical representation of all considered methodologies, namely Objective Reinforced Generative Adversarial Network<sup>40</sup> (ORGAN), Objective Reinforced



Generative Adversarial Network for Inverse-Design Chemistry<sup>32</sup> (ORGANIC), Conditional Diversity Network<sup>24</sup> (CDN), Variational Autoencoder with Multilayer Perceptron<sup>41</sup> (ChemVAE), Grammar Variational Autoencoder<sup>42</sup> (GrammarVAE), Conditional Variational Autoencoder<sup>37</sup> (CVAE), Recurrent Neural Networks<sup>43</sup> (RNN), Junction Tree Variational Autoencoder<sup>39</sup> (JT-VAE), a CycleGAN<sup>44</sup> based model<sup>45</sup> (MolCycleGAN) and Semi Supervised Variational Autoencoder<sup>46</sup> (SSVAE), can be seen in Fig. 1.

**1.4.1 Autoencoder-based methods.** CDN is a deep learning network that utilizes a variational auto-encoder (VAE) with a “diversity” layer to generate molecules that are similar to the prototype, yet different. To do this they introduce the diversity layer to the vanilla VAE architecture. So, during the generation stage instead of using random noise as an input to the decoder, the CDN uses a sample of the prototype as an input to the decoder. This allows sampling molecules that have similar features when compared to the prototype.

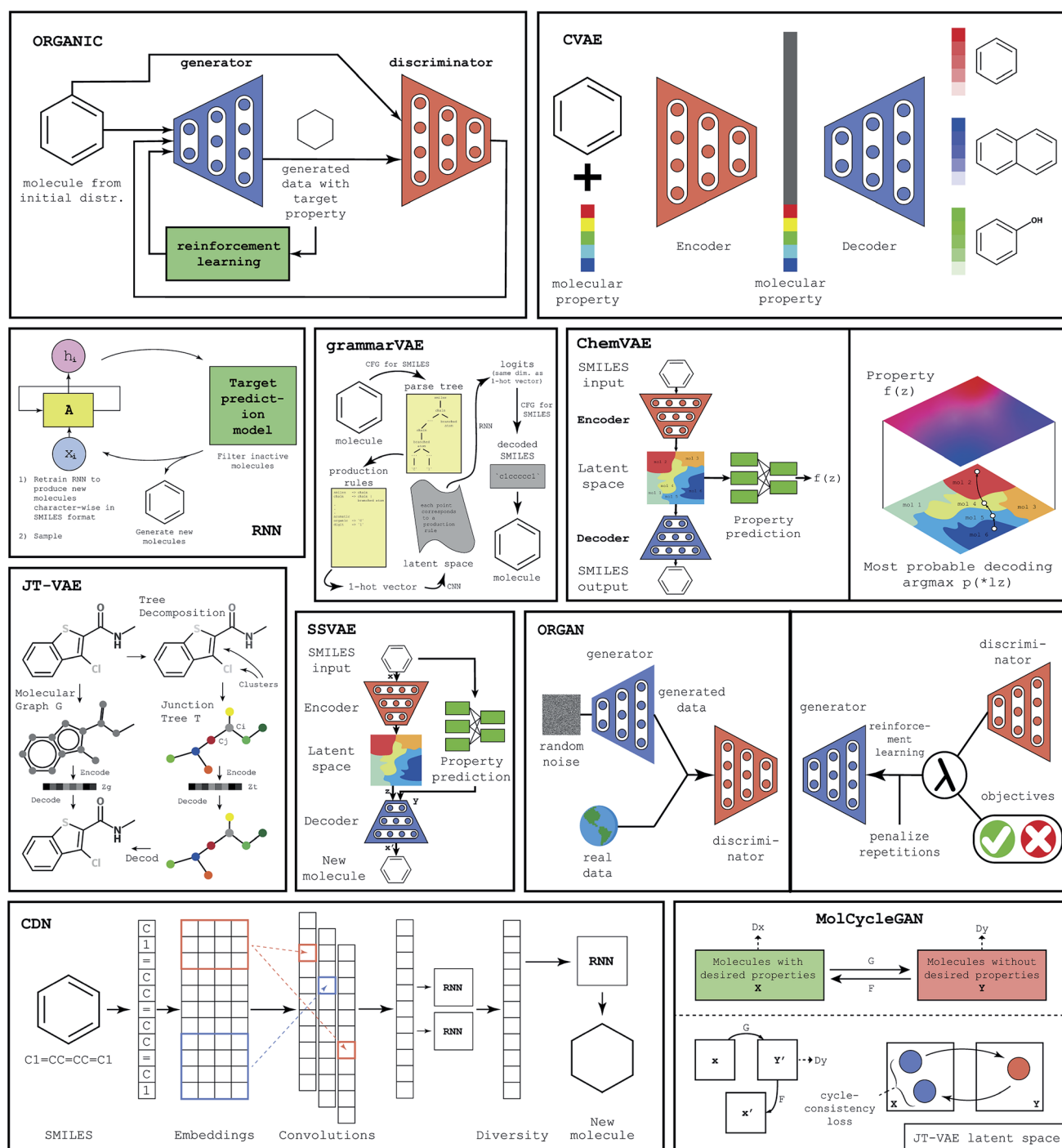


Fig. 1 The graphical representations of machine learning algorithms used to create the database.

ChemVAE is an autoencoder with a multilayer perceptron that is used for property prediction. While the autoencoder is employed to learn the latent space of valid molecules, the multilayer perceptron is used to generate molecules with desired properties. Trained jointly with the autoencoder, the perceptron organizes the latent space, grouping the molecules with similar property values in the same latent region. This allows the sampling of molecules with desired properties.

While methods like ORGAN or ORGANIC use a GAN and RNN to generate sequence data like the SMILES molecule representation, GrammarVAE attempts to avoid learning the syntax of the SMILES. Instead of having a GAN learn the syntax of the SMILES format, GrammarVAE uses the fact that SMILES can be represented by context-free grammar and learns the grammar rules, thus avoiding the generation of molecules that are syntactically invalid. To do this GrammarVAE calculates the parsing tree of a molecule, then converts it into one-hot-encoding, having the variational autoencoder learn the sequence of applied grammar rules, rather than individual characters.

JT-VAE deviates from the traditional approach to molecule generation. Instead of using the SMILES representation of the molecule, JT-VAE utilizes direct graph representation of the molecule. JT-VAE builds new molecules by using subgraphs of the old ones. While other methods often use atom combination approach, the JT-VAE uses component combination. Combination of the graph representation and the variational autoencoder almost always yields valid molecules. CVAE is aimed to generate molecules with several desired properties. It was observed that optimization for one property may unintentionally change other properties. In order to counter this effect, CVAE is designed as an artificial neural network that is suitable for optimization of multiple properties. To achieve this goal CVAE uses a conditional vector for both encoding and decoding. Such an architecture allows for the incorporation of properties into the latent space.

**1.4.2 RNN-based methods.** In this method, RNN is represented by long term short memory (LSTM). The architecture is comprised of 3 stacked LSTM layers. To overcome the problem of generating unfocused molecules, transfer learning is employed. After transfer learning, a small subset of the focused molecules is used to fine-tune the model, so that it generates molecules with desired properties.

SSVAE is a semi supervised model that has advantages when dealing with datasets where only a part of the dataset is labeled with properties. It consists of 3 bi-directional RNNs, which are used for encoding, decoding, and predicting. In this model, the property prediction and molecule generation are combined in a single network. The novel molecules are decoded from the latent space, which is the product of the trained encoder.

**1.4.3 GAN-based methods.** ORGAN is an artificial neural network architecture based on SeqGAN,<sup>47</sup> which is adapted for melody and molecule generation. It feeds SMILES molecules to the generative network of the GAN and uses Wasserstein-1 distance to improve the results of the training.

ORGANIC is a framework for the generation of novel molecules, which is based on ORGAN. It is a more chemistry oriented version of ORGAN. The limitation of the ORGANIC is that it has

an unstable output of molecules. The range of invalid molecules that are created deviates between 0.2 and 99 percent.

MolCycleGAN is based on the CycleGAN. To generate novel molecules with similar properties MolCycleGAN uses JT-VAE as a latent space producer, then utilizes GAN to produce the molecule. To feed the GAN a molecule with desired features is used and the resultant latent space embedding is then transformed back to the new molecule with a similar structure and desired properties.

## 2 System overview

### 2.1 Implementation of methods

Implementations of each method aside from RNN<sup>48</sup> were mentioned in the original publications. All of the algorithms were written in Python with the help of either Pytorch<sup>49</sup> or Tensorflow.<sup>50</sup> Training of all the methods except for RNN was conducted using the samples of molecules from ZINC that were provided by the authors of the original implementations. For RNN we have used a ZINC-based training dataset, which was provided by the authors of JT-VAE.<sup>39</sup> In addition, we ran implementations of CDN and RNN methods utilizing a 1.6 million molecules sample of ChEMBL<sup>51</sup> as a training dataset. As a result, *ca.* 0.62 thousand out of the total 3.64 thousand molecules generated with CDN and *ca.* 0.65 million out of the total 0.96 million molecules generated with RNN were obtained based on the ChEMBL training data.

### 2.2 Molecule storage and preprocessing

All generated molecules along with their properties are stored in PostgreSQL, a free and open-source relational database management system with a variety of modules that allows to use them in different contexts. For instance, RDKit Cartridge enables efficient search across molecules.

Preprocessing is an important step in the management of a large molecular database, containing millions of members. Utilizing RDKit<sup>52</sup> 2.9 million molecules, produced by the above mentioned generative ML algorithms, were inserted into the database in canonical SMILES format. During the insertion a fraction of molecules were discarded: 174 000 were invalid (according to RDKit) and for 633 RDKit was not able to construct canonical SMILES. In addition, all duplicates were removed. In total, 2.8 million molecules were inserted along with computed properties that are listed in Lipinski's rule of five.<sup>53</sup> Moreover, we have computed other medicinal chemistry-relevant properties such as the number of rotatable bonds and the number of saturated rings.

The typical operations on databases composed of a large number of molecules involve searching by substructure and searching by similarity. To optimize such queries we have pre-computed Morgan Fingerprints (Circular Fingerprints) as well as the RDKit implementation of Extended Connectivity Fingerprints.<sup>54</sup>

### 2.3 Searching molecules

Fig. 2 demonstrates two pages of the application: "draw molecule" and "query results". The "draw molecule" page has





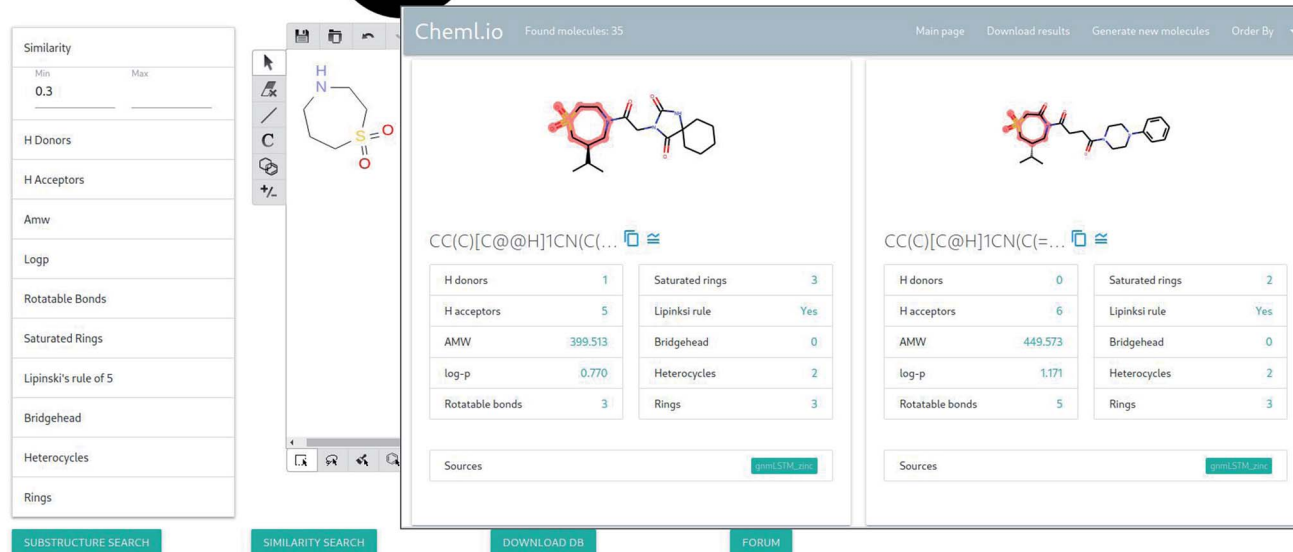


Fig. 2 The screenshots of two main pages of the application.

a doodle widget that allows drawing molecules using common tools, such as bonds, atoms, ring tools, among others, and uses this information as an input for the query. This widget is adopted from an open-source javascript library called *Kekule.js*.<sup>55</sup> The “query results” page lists molecules with some common properties that satisfy the given query. The resulting molecules can be sorted based on a range of molecular properties. In addition, the results can be downloaded as a csv file containing the molecules in SMILES format. Furthermore, the interface allows opting for the generation of additional molecules that are either similar to the original query or to any of the molecules retrieved from the database.

There are two types of queries: substructure search and similarity search. The substructure search performs the following operation:

Given a molecule X in SMILES format, find all molecules that contain X.

The similarity search performs the following operation:

Given a similarity threshold  $\varepsilon$ , find all molecules Y s.t. the  $\text{dist}(X, Y) < \varepsilon$ , where the  $\text{dist}(\cdot, \cdot)$  is the Tanimoto distance<sup>56</sup>.

By specifying the upper and lower bounds of molecular properties, it is possible to narrow down the search results.

## 2.4 Generation on demand

Currently, we employ Conditional Diversity Networks<sup>24</sup> for the generation of new molecules on demand. Based on our observations, the algorithm achieves the best results when the training is performed for each request. Our current approach can be summarized as follows:

1. Fetch molecules that are similar to the seed molecule from three databases: ZINC,<sup>57</sup> ChEMBL<sup>51</sup> and cheML.
2. Utilize these molecules as input data for the first training.

Table 1 Qualitative comparison of the algorithms

Model	Architecture	Learning technique	Molecule representation	Property targeting	Computational costs	Training dataset size
JT-VAE	VAE	Autoencoder	Graph	Yes	Medium	250k
RNN	RNN	Direct flow	SMILES	No	Low	250k
GrammarVAE	VAE	Autoencoder	SMILES	No	High	250k
ChemVAE	VAE	Autoencoder	SMILES	Yes	Medium	250k
MolCycleGan	GAN	Direct flow	Latent vector	Yes	Medium	250k
ORGAN	GAN	RL	SMILES	Yes	High	1 million
ORGANIC	GAN	RL	SMILES	Yes	High	250k
SSVAE	VAE	Autoencoder	SMILES	Yes	Medium	310k
CDN	VAE	Autoencoder	SMILES	No	Low	250k
CVAE	VAE	Autoencoder	SMILES	Yes	Medium	500k



- Fetch molecules from the above databases that contain the seed molecule as a substructure.
- Utilize these molecules as input data for the second training.
- Combine previous input data and use them as input for a third training.
- Generate molecules using all three distinct models built by each of the above input data. Filter the resulting molecules based on their similarity score with the seed molecule. Exclude the molecules that are already present in the cheML.io database and those featuring the same structural backbone (*i.e.* different only by the stereochemical features) and send the outcome to the user by email.
- Add novel molecules to the cheML.io database.

## 3 Results and discussion

### 3.1 Key characteristics of methods

To compare methods that were employed for the generation of molecules, we have looked into the several key characteristics of the machine learning algorithms: architecture, learning technique, molecular representations used, whether it can target desired property, computational resources needed to run it, and size of the training dataset. Please refer to the Table 1 for an overview.

### 3.2 Analysis across methods

As can be seen in Fig. 3, we did not aim to create a uniform number of molecules per method when implementing the studied algorithms. The main reason is due to the fact that some of the algorithms are more suitable for the generation of

the bulk of molecules while others are more convenient for the targeted generation of specific molecules. For example, CVAE can be regarded as a specialized algorithm for the generation of molecules displaying specific properties while CDN is designed to generate similar yet diverse molecules when compared to a particular prototype. Thus, both CVAE and CDN were deployed by us for the generation of only a relatively small set of molecules ranging from several hundred to several thousand. On the other hand, considering its focus on structural similarity, CDN appeared to be the most suitable method for incorporating it into the generation on demand feature.

While the majority of generation algorithms shows a rather diverse output, when compared to the output of other algorithms (see Fig. 3), 49.07% of molecules generated by MolCycleGAN were also generated by GrammarVAE. This indicates that these methods may have a similar latent space despite that MolCycleGAN uses direct graph representation of the molecule while GrammarVAE uses the context-free grammar of the SMILES representation.

To further validate and compare the effectiveness of the implemented algorithms, metrics from the MOSES benchmarking framework<sup>58</sup> were employed. Using the provided toolbox, we have calculated several representative metrics including novelty, internal diversity, and medical filters. Comparing the obtained results with the benchmark baselines indicates that almost all the methods demonstrated decent performance (see ESI for details†).

### 3.3 Diversity analysis

**3.3.1 Comparison of large-scale databases.** In order to assess the molecular diversity of the cheML.io database we

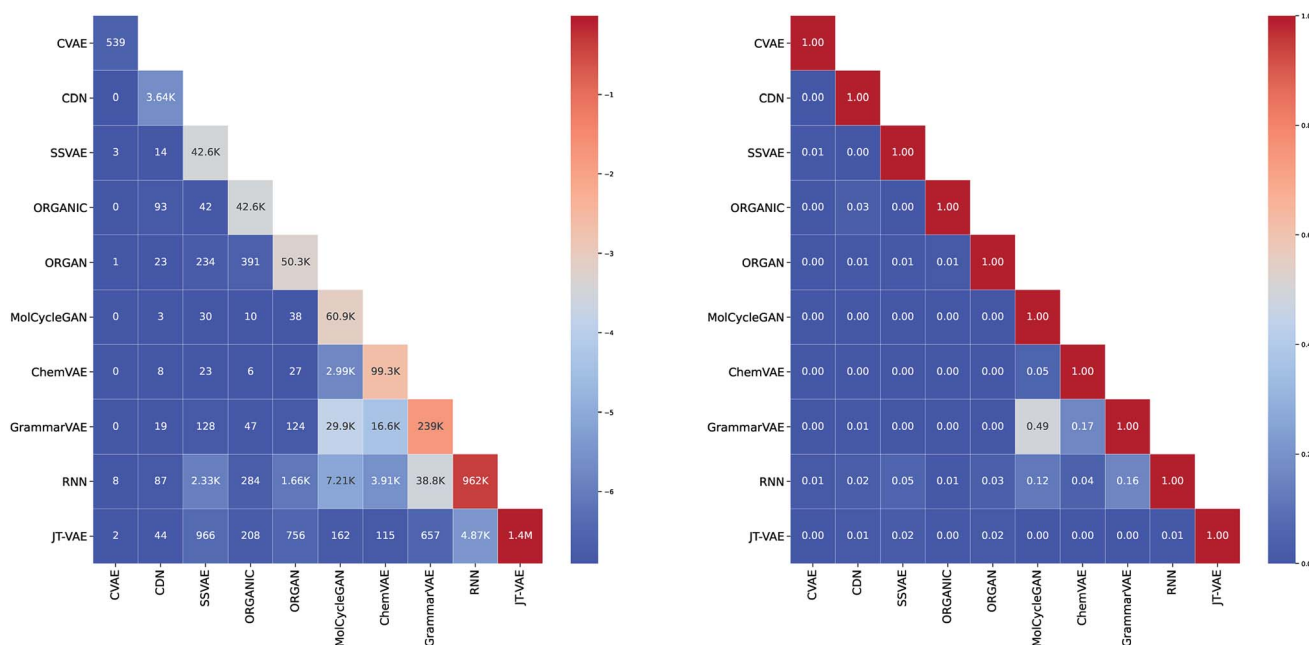


Fig. 3 (Left) The diagonal of the matrix illustrates total number of molecules generated by each method. Intersections below the diagonal show number of same molecules that were generated by both methods. (Right) Each entry shows the proportion of shared molecules between each method.



decided to perform an inter-database comparison with eMolecules<sup>59</sup> as well as ZINC.<sup>57</sup> Both databases comprise an extensive set of available chemical compounds on the market. eMolecules contains 26.4 million molecules while ZINC contains over 750 million molecules. Therefore, we have opted to perform the comparison with a fraction of ZINC instead of utilizing the whole database. To uniformly sample and minimize the probability of obtaining a biased subset, we sampled 1.5 million ZINC molecules 20 times. All molecules were sampled from the lead-like molecules subset of ZINC. The means and standard deviations of the molecular properties were statistically examined across all 20 samples and no significant variations were identified and thereby we assumed that these samples are representative of the whole ZINC database. As a final step, all 20 samples were merged to create a subset of 30 million ZINC molecules, which was used for all future comparisons. The comparison was performed using the following methodology:

- Calculate a number of key molecular properties and structural parameters including molecular mass, number of atoms, number of chiral centers, number of rings, number of bridgehead atoms and number of heterocycles for the molecules from cheML, eMolecules and ZINC databases, as well as subsets of ML model outputs.
- Calculate the mean and standard deviation across above properties for each database, and subsets of cheML.
- Conduct statistical analyses to assess how the data fit the normal and uniform distributions property-wise; whether the variances across each property are equal between the databases; and whether the distributions of the data are somewhat similar between cheML.io and ZINC.

When comparing cheML.io with eMolecules and ZINC our database contains more diverse molecules across properties such as molecular mass and number of atoms, while the eMolecules database is the most diverse in terms of the number of rings and heterocycles. ZINC has the most variance for the number of chiral centers and bridgehead atoms (see Table 2).

A test of normality was performed, which is based on D'Agostino and Pearson's test that combines skew and kurtosis to produce an omnibus test of normality.<sup>60,61</sup> Our results indicate that all three databases' data are not normal for the considered properties. The implementation of the SciPy package was used for this and following statistical tests.<sup>62</sup> Levene's test, which is optimal for highly non-normal data, showed that all property-wise differences in variances are statistically significant. This solidifies the claims stated in the previous paragraph. Lastly, a two-sample Kolmogorov-Smirnov test revealed that the distribution of values is not equal when comparing cheML.io with and the two other databases. This holds true for each property.

**3.3.2 Comparison of CheML constituents.** The number of generated molecules as well as the key molecular properties of each ML model output are presented in Table 2. It is evident that the properties of molecules in CheML vary dramatically depending on the ML algorithm used. For instance, RNN has an extremely high mean and variance in Exact molecular mass, which together with the fact that this subset constitutes about 1/3 of CheML, results in a very high variance in CheML's Exact molecular mass overall.

To compare ZINC and CheML side-by-side, normality tests were performed (based on D'Agostino and Pearson's test that combines skew and kurtosis to produce an omnibus test of normality) in order to determine the appropriate statistical tests for comparing variances and distributions. The normality tests indicated that most methods produce non-normal distributions with a significance level of  $\alpha = 0.001$ . Please note that all  $p$ -values were corrected for multiple testing by application of Bonferroni correction.<sup>63</sup> The only tests where the normality hypothesis could not be rejected were CheML CVAE for the properties: exact molecular weight, number of atoms, and number of rings.

The Kolmogorov-Smirnov test was used to deduce that the outputs of all models are statistically significantly different

Table 2 General information about the three databases

Database	Number of molecules	Exact molecular mass	Number of atoms	Number of chiral centers	Number of rings	Number of bridgehead atoms	Number of heterocycles
CheML	2 899 276	373 $\pm$ 213	26.3 $\pm$ 15	0.23 $\pm$ 0.60	2.55 $\pm$ 1.02	0.023 $\pm$ 0.248	1.18 $\pm$ 0.93
eMolecules	26 394 586	331 $\pm$ 87.7	22.8 $\pm$ 6.46	0.0944 $\pm$ 0.489	2.63 $\pm$ 1.16	0.036 $\pm$ 0.319	1.35 $\pm$ 0.97
ZINC	30 000 000	321 $\pm$ 24.5	22.7 $\pm$ 2.0	1.399 $\pm$ 1.017	2.55 $\pm$ 0.90	0.076 $\pm$ 0.391	1.72 $\pm$ 0.95
CheML JT-VAE	1 399 265	323 $\pm$ 55	22.7 $\pm$ 3.9	0.0 $\pm$ 0.0	2.69 $\pm$ 0.93	0.024 $\pm$ 0.25	1.41 $\pm$ 0.89
CheML RNN	962 245	475 $\pm$ 336	33.8 $\pm$ 23.8	0.30 $\pm$ 0.66	2.37 $\pm$ 1.12	0.0176 $\pm$ 0.23	0.80 $\pm$ 0.84
CheML	239 206	326 $\pm$ 59	22.7 $\pm$ 4.25	0.86 $\pm$ 0.90	2.63 $\pm$ 0.93	0.0238 $\pm$ 0.247	1.37 $\pm$ 0.92
GrammarVAE							
CheML	99 273	333 $\pm$ 63	22.9 $\pm$ 4.6	0.81 $\pm$ 0.9	2.72 $\pm$ 1.01	0.0540 $\pm$ 0.37	1.48 $\pm$ 0.95
ChemVAE							
CheML	60 856	330 $\pm$ 61	23.0 $\pm$ 4.4	0.94 $\pm$ 1.00	2.75 $\pm$ 0.98	0.0400 $\pm$ 0.32	1.45 $\pm$ 0.96
MolCycleGAN							
CheML ORGAN	50 262	273 $\pm$ 58	18.6 $\pm$ 4.1	0.28 $\pm$ 0.57	2.20 $\pm$ 0.75	0.029 $\pm$ 0.26	0.77 $\pm$ 0.72
CheML	42 609	222 $\pm$ 60	15.8 $\pm$ 4.39	0.74 $\pm$ 0.82	1.39 $\pm$ 0.58	0.0022 $\pm$ 0.068	0.46 $\pm$ 0.55
ORGANIC							
CheML SSSVAE	42 606	355 $\pm$ 70	24.9 $\pm$ 4.8	0.0 $\pm$ 0.0	2.89 $\pm$ 0.92	0.034 $\pm$ 0.26	1.18 $\pm$ 0.87
CheML CDN	2415	385 $\pm$ 413	26.8 $\pm$ 27.8	0.44 $\pm$ 0.74	2.70 $\pm$ 1.28	0.167 $\pm$ 0.7	1.35 $\pm$ 1.07
CheML CVAE	539	304 $\pm$ 19	22.3 $\pm$ 1.48	0.87 $\pm$ 1.26	2.19 $\pm$ 0.52	0.0074 $\pm$ 0.122	0.69 $\pm$ 0.69



from uniform distributions along any property. Levene tests for equal variances yielded that variances vary statistically significantly when comparing the ML model outputs with the ZINC sample for all 6 molecular properties, which can be seen in Table 2. The only exception, where the null hypothesis of equal variance could not be rejected was for CheML CVAE *vs.* ZINC for the number of chiral centers. Two-sample Kolmogorov–Smirnov test indicates that the difference between ML model outputs and ZINC sample is statistically significant across all properties, with only two exceptions being CheML CVAE *vs.* ZINC for the number of bridgehead atoms and CheML CVAE *vs.* ZINC for the same property.

According to the vast majority of tests, variances and distributions are not equal when comparing ML model outputs to the ZINC sample. Out of 120 statistical tests between CheML and ZINC in total, 117 yielded statistical significance. It is important to note that the CheML CVAE sub-dataset which constituted 2 out of 3 tests where the null hypothesis could not be rejected, is also the smallest set among the outputs, comprising only 539 molecules.

In addition, further statistical tests were performed, where each of the molecular properties' variances were compared utilizing Levene's test across all considered methods. Also, Kolmogorov–Smirnov tests were applied for testing equal distributions. These results can be obtained from Tables S2 and S3 in ESI.†

### 3.4 Performance of generation on demand

As was mentioned in the system overview section, we use the CDN as an algorithm for the generation of molecules on demand. To improve the proportion of correctly generated molecules we have substituted the SMILES character parser to a SMILES grammar parser. The original method of converting SMILES strings to number vectors involved assigning a number to each character of the SMILES string. For example, the atom H would be codified as 23, atom S as 24 and atom Si as a combination of two numbers 24 and 25 that should be placed consecutively.

Thus, if number 25 would appear as standalone in the resulting vector, the whole vector would be discarded because the corresponding string and associated molecule would be invalid. To eliminate such cases we have used the SMILES grammar parser that breaks the SMILES string into morphemes, *i.e.* atoms and supporting elements, like stereoisomers. While the grammar parser does not eliminate syntactic errors it helps with standalone atom parts.

Utilizing the uniform training dataset for every generation request mainly resulted in a production of completely irrelevant molecules. However, when we have introduced the application of case specific training datasets described in the previous section the reliability of generation on demand feature has greatly improved.

During testing, we have observed that all the inputs for the generation on demand could be roughly divided into three categories: small molecules representing common structural motifs widely found in more complex molecules, medium-sized molecules that are not so widespread as subunits for other

molecules, and large complex molecules that cannot be identified as substructures of any molecules from ZINC, ChEMBL or cheML.io. Owing to these differences, inputs from each of the above categories might require their own approach for assembling the training datasets. For example, the similarity-based training dataset for small molecules could be readily assembled from any database. However, due to the small size of the input molecule, the resulting training dataset might include molecules that are rather different from the initial one in the sense that they would not contain it as a substructure. Thus, adding a substructure-based training dataset and blending it with a similarity-based training dataset has generally led to a more balanced outcome for the generation requests featuring small and medium-sized molecules as inputs. On the other hand, for large and complex molecules that can not be found as substructures of other molecules, the only option is to use a similarity-based training dataset. Therefore, we have designed a 3-stage process for assembling the training datasets that accounts for the above mentioned variations and provides optimal results for any type of input structure without the need for manual categorizing.

## 4 Conclusions

In summary, we have surveyed and tested a number of ML algorithms for the *de novo* generation of organic molecules. A database of 2.8 million molecules originating from these efforts has been integrated into a user-friendly webpage framework that allows to perform substructure and similarity searches and browse the results in an interactive fashion. To facilitate and structurize the browsing process all the molecules in the database have been supplemented with a range of calculated molecular properties and structural features. Thus, the outcome of every search can be ordered, based on the chosen property or structural parameter. In addition, the molecules resulting from each specific search request as well as the overall database can be readily retrieved in a csv file, where molecules appear in SMILES format. When a specific search leads to insufficient results, users are able to request the generation of new molecules with the aid of the Conditional Diversity Network (CDN) algorithm. The user can opt to generate the molecules that are either similar to the original input structure or to any of the molecules retrieved from the database. All the newly generated molecules will be directly incorporated into the database assuring its continuous broadening and improvement. The generation on demand feature will also undergo further tuning and enhancement. In order to facilitate this process, the users will be provided with the possibility to leave their feedback and suggestions.

We hope this dynamic online database may eventually provide assistance to researchers that are interested in the biological validation of ML-generated molecules and thereby justify the means of creating them.

## Conflicts of interest

There are no conflicts to declare.





## Acknowledgements

This research was supported by Nazarbayev University Faculty Development Grant (240919FD3926). The authors would also like to acknowledge the support of NPO Young Researchers Alliance and Nazarbayev University Corporate Fund "Social Development Fund" for grant under their Fostering Research and Innovation Potential Program.

## Notes and references

- 1 N. R. Council, *Beyond the Molecular Frontier: Challenges for Chemistry and Chemical Engineering*, The National Academies Press, Washington, DC, 2003.
- 2 W. H. Sauer and M. K. Schwarz, *J. Chem. Inf. Comput. Sci.*, 2003, **43**, 987.
- 3 S. L. Schreiber, *Nature*, 2009, **457**, 153.
- 4 S. Dandapani and L. A. Marcaurelle, *Nat. Chem. Biol.*, 2010, **6**, 861.
- 5 S. Wu, Y. Kondo, M.-a. Kakimoto, B. Yang, H. Yamada, I. Kuwajima, G. Lambard, K. Hongo, Y. Xu, J. Shiomi, C. Schick, J. Morikawa and R. Yoshida, *npj Comput. Mater.*, 2019, **5**, 66.
- 6 R. S. Bohacek, C. McMartin and W. C. Guida, *Med. Res. Rev.*, 1996, **16**, 3.
- 7 P. G. Polishchuk, T. I. Madzhidov and A. Varnek, *J. Comput.-Aided Mol. Des.*, 2013, **27**, 675.
- 8 B. K. Shoichet, *Nature*, 2004, **432**, 862.
- 9 S. Ghosh, A. Nie, J. An and Z. Huang, *Curr. Opin. Chem. Biol.*, 2006, **10**, 194.
- 10 D. Stumpfe and J. Bajorath, *Wiley Interdiscip. Rev.: Comput. Mol. Sci.*, 2011, **1**, 260.
- 11 G. Schneider and U. Fechner, *Nat. Rev. Drug Discovery*, 2005, **4**, 649.
- 12 A. M. Virshup, J. Contreras-García, P. Wipf, W. Yang and D. N. Beratan, *J. Am. Chem. Soc.*, 2013, **135**, 7296.
- 13 A. Kadurin, A. Aliper, A. Kazennov, P. Mamoshina, Q. Vanhaelen, K. Khrabrov and A. Zhavoronkov, *Oncotarget*, 2017, **8**, 10883.
- 14 B. Sanchez-Lengeling and A. Aspuru-Guzik, *Science*, 2018, **361**, 360.
- 15 D. C. Elton, Z. Boukouvalas, M. D. Fuge and P. W. Chung, *Mol. Syst. Des. Eng.*, 2019, **4**, 828.
- 16 G. Chen, Z. Shen, A. Iyer, U. F. Ghumman, S. Tang, J. Bi, W. Chen and Y. Li, *Polymers*, 2020, **12**, 163.
- 17 N. Brown, P. Ertl, R. Lewis, T. Luksch, D. Reker and N. Schneider, *J. Comput.-Aided Mol. Des.*, 2020, **34**, 709.
- 18 *Cheml.io*, accessed September 2020, <https://cheml.io>.
- 19 A. Zhavoronkov, Y. A. Ivanenkov, A. Aliper, M. S. Veselov, V. A. Aladinskiy, A. V. Aladinskaya, V. A. Terentiev, D. A. Polykovskiy, M. D. Kuznetsov, A. Asadulaev, Y. Volkov, A. Zholus, R. R. Shayakhmetov, A. Zhebrak, L. I. Minaeva, B. A. Zagribelnyy, L. H. Lee, R. Soll, D. Madge, L. Xing, T. Guo and A. Aspuru-Guzik, *Nat. Biotechnol.*, 2019, **37**, 1038.
- 20 Y. Le Cun and F. Fogelman-Soulié, *Intellectica*, 1987, **1**, 114.
- 21 D. E. Rumelhart, G. E. Hinton and R. J. Williams, *Nature*, 1986, **323**, 533.
- 22 I. J. Goodfellow, J. Pouget-Abadie, M. Mirza, B. Xu, D. Warde-Farley, S. Ozair, A. Courville and Y. Bengio, *Proceedings of the 27th International Conference on Neural Information Processing Systems - Volume 2*, ed. Z. Ghahramani, M. Welling, C. Cortes, N. D. Lawrence and K. Q. Weinberger, MIT Press, Cambridge, MA, USA, 2014, p. 2672.
- 23 I. Goodfellow, Y. Bengio and A. Courville, *Deep learning*, The MIT Press, Cambridge, Massachusetts, 2016.
- 24 S. Harel and K. Radinsky, *Proceedings of the 24th ACM SIGKDD International Conference on Knowledge Discovery & Data Mining - KDD '18*, London, United Kingdom, 2018, p. 331.
- 25 H. Zhang, T. Xu, H. Li, S. Zhang, X. Wang, X. Huang and D. Metaxas, *2017 IEEE International Conference on Computer Vision (ICCV)*, 2017, p. 5908.
- 26 C. Ledig, L. Theis, F. Huszár, J. Caballero, A. Cunningham, A. Acosta, A. Aitken, A. Tejani, J. Totz, Z. Wang and W. Shi, *2017 IEEE Conference on Computer Vision and Pattern Recognition (CVPR)*, 2017, p. 105.
- 27 C. Vondrick, H. Pirsiavash and A. Torralba, *Proceedings of the 30th International Conference on Neural Information Processing Systems*, Red Hook, NY, USA, 2016, p. 613.
- 28 L.-C. Yang, S.-Y. Chou and Y.-H. Yang, *Proceedings of the 18th International Society for Music Information Retrieval Conference, ISMIR 2017*, Suzhou, China, October 23-27, 2017, p. 324.
- 29 T. Schlegl, P. Seeböck, S. M. Waldstein, U. Schmidt-Erfurth and G. Langs, *Information Processing in Medical Imaging*, ed. M. Niethammer, M. Styner, S. Aylward, H. Zhu, I. Oguz, P.-T. Yap and D. Shen, Springer International Publishing, Cham, 2017, vol. 10265, p. 146.
- 30 N. Killoran, L. J. Lee, A. Delong, D. Duvenaud and B. J. Frey, *arXiv*, 2017, preprint, arXiv:1712.06148v1, <https://arxiv.org/abs/1712.06148v1>.
- 31 A. Kadurin, S. Nikolenko, K. Khrabrov, A. Aliper and A. Zhavoronkov, *Mol. Pharm.*, 2017, **14**, 3098.
- 32 B. Sanchez-Lengeling, C. Outeiral, G. L. Guimaraes and A. Aspuru-Guzik, *ChemRxiv*, 2017, DOI: 10.26434/chemrxiv.5309668.v3, preprint.
- 33 L. David, A. Thakkar, R. Mercado and O. Engkvist, *J. Cheminf.*, 2020, **12**, 56.
- 34 D. Weininger, *J. Chem. Inf. Comput. Sci.*, 1988, **28**, 31.
- 35 J. W. Raymond and P. Willett, *J. Comput.-Aided Mol. Des.*, 2002, **16**, 521.
- 36 A. Cadeddu, E. K. Wylie, J. Jurczak, M. Wampler-Doty and B. A. Grzybowski, *Angew. Chem., Int. Ed.*, 2014, **53**, 8108.
- 37 J. Lim, S. Ryu, J. W. Kim and W. Y. Kim, *J. Cheminf.*, 2018, **10**, 31.
- 38 T. Blaschke, O. Engkvist, J. Bajorath and H. Chen, *J. Cheminf.*, 2020, **12**, 68.
- 39 W. Jin, R. Barzilay and T. Jaakkola, *Proceedings of the 35th International Conference on Machine Learning*, Stockholm, Sweden, 2018, p. 2323.
- 40 G. L. Guimaraes, B. Sanchez-Lengeling, C. Outeiral, P. L. C. Farias and A. Aspuru-Guzik, *arXiv*, 2018,



- preprint, arXiv:1705.10843v3, <https://arxiv.org/abs/1705.10843v3>.
- 41 R. Gómez-Bombarelli, J. N. Wei, D. Duvenaud, J. M. Hernández-Lobato, B. Sánchez-Lengeling, D. Sheberla, J. Aguilera-Iparraguirre, T. D. Hirzel, R. P. Adams and A. Aspuru-Guzik, *ACS Cent. Sci.*, 2018, **4**, 268.
  - 42 M. J. Kusner, B. Paige and J. M. Hernández-Lobato, *Proceedings of the 34th International Conference on Machine Learning-Volume 70*, 2017, p. 1945.
  - 43 M. H. S. Segler, T. Kogej, C. Tyrchan and M. P. Waller, *ACS Cent. Sci.*, 2018, **4**, 120.
  - 44 J.-Y. Zhu, T. Park, P. Isola and A. A. Efros, *2017 IEEE International Conference On Computer Vision (ICCV)*, 2017, p. 2242.
  - 45 Ł. Maziarka, A. Pocha, J. Kaczmarczyk, K. Rataj and M. Warchoń, *Artificial Neural Networks and Machine Learning – ICANN 2019, Workshop and Special Sessions*, Cham, 2019, p. 810.
  - 46 S. Kang and K. Cho, *J. Chem. Inf. Model.*, 2019, **59**, 43.
  - 47 L. Yu, W. Zhang, J. Wang and Y. Yu, *Proceedings of the Thirty-First AAAI Conference on Artificial Intelligence*, San Francisco, California, USA, 2017, p. 2852.
  - 48 Implementation of RNN from <https://github.com/LamUong/Generate-novel-molecules-with-LSTM> was used.
  - 49 A. Paszke, S. Gross, F. Massa, A. Lerer, J. Bradbury, G. Chanan, T. Killeen, Z. Lin, N. Gimelshein, L. Antiga, A. Desmaison, A. Kopf, E. Yang, Z. DeVito, M. Raison, A. Tejani, S. Chilamkurthy, B. Steiner, L. Fang, J. Bai and S. Chintala, *Advances in Neural Information Processing Systems 32*, ed. H. Wallach, H. Larochelle, A. Beygelzimer, F. dAlché-Buc, E. Fox and R. Garnett, Curran Associates, Inc., Red Hook, NY, USA, 2019, p. 8024.
  - 50 M. Abadi, P. Barham, J. Chen, Z. Chen, A. Davis, J. Dean, M. Devin, S. Ghemawat, G. Irving, M. Isard, M. Kudlur, J. Levenberg, R. Monga, S. Moore, D. G. Murray, B. Steiner, P. Tucker, V. Vasudevan, P. Warden, M. Wicke, Y. Yu and X. Zheng, *Proceedings of the 12th USENIX Conference on Operating Systems Design and Implementation*, USA, 2016.
  - 51 D. Mendez, A. Gaulton, A. P. Bento, J. Chambers, M. De Veij, E. Félix, M. P. Magariños, J. F. Mosquera, P. Mutowo, M. Nowotka, M. Gordillo-Marañón, F. Hunter, L. Junco, G. Mugumbate, M. Rodriguez-Lopez, F. Atkinson, N. Bosc, C. J. Radoux, A. Segura-Cabrera, A. Hersey and A. R. Leach, *Nucleic Acids Res.*, 2018, **47**, D930.
  - 52 RDKit: *Open-source cheminformatics*, accessed September 2020, <http://www.rdkit.org>.
  - 53 C. A. Lipinski, F. Lombardo, B. W. Dominy and P. J. Feeney, *Adv. Drug Delivery Rev.*, 1997, **23**, 3.
  - 54 D. Rogers and M. Hahn, *J. Chem. Inf. Model.*, 2010, **50**, 742.
  - 55 C. Jiang, X. Jin, Y. Dong and M. Chen, *J. Chem. Inf. Model.*, 2016, **56**, 1132.
  - 56 G. Maggiora, M. Vogt, D. Stumpfe and J. Bajorath, *J. Med. Chem.*, 2014, **57**, 3186.
  - 57 T. Sterling and J. J. Irwin, *J. Chem. Inf. Model.*, 2015, **55**, 2324.
  - 58 D. Polykovskiy, A. Zhebrak, B. Sanchez-Lengeling, S. Golovanov, O. Tatanov, S. Belyaev, R. Kurbanov, A. Artamonov, V. Aladinskiy, M. Veselov, A. Kadurin, S. Johansson, H. Chen, S. Nikolenko, A. Aspuru-Guzik and A. Zhavoronkov, arXiv, 2020, preprint, arXiv:1811.12823v5, <https://arxiv.org/abs/1811.12823v5>.
  - 59 eMolecules, <https://www.emolecules.com/info/products-data-downloads.html>, accessed September 2020.
  - 60 R. d'Agostino, *Biometrika*, 1971, **58**, 341.
  - 61 R. d'Agostino and E. S. Pearson, *Biometrika*, 1973, **60**, 613.
  - 62 P. Virtanen, R. Gommers, T. E. Oliphant, M. Haberland, T. Reddy, D. Cournapeau, E. Burovski, P. Peterson, W. Weckesser, J. Bright, S. J. van der Walt, M. Brett, J. Wilson, K. Jarrod Millman, N. Mayorov, A. R. J. Nelson, E. Jones, R. Kern, E. Larson, C. Carey, Í. Polat, Y. Feng, E. W. Moore, J. Vand erPlas, D. Laxalde, J. Perktold, R. Cimrman, I. Henriksen, E. A. Quintero, C. R. Harris, A. M. Archibald, A. H. Ribeiro, F. Pedregosa, P. van Mulbregt and SciPy 1.0 Contributors, *Nat. Methods*, 2020, **17**, 261.
  - 63 C. Bonferroni, *Pubblicazioni del R Istituto Superiore di Scienze Economiche e Commerciali di Firenze*, 1936, **8**, p. 3.

